Pyrenyl-Functionalized Fluorene and Carbazole Derivatives as Blue Light Emitters

ARTICLE · APRIL 2012

DOI: 10.1021/jp300161k

7 AUTHORS, INCLUDING:

Simonas Krotkus
Technische Universität Dresden
7 PUBLICATIONS **58** CITATIONS
SEE PROFILE

Arunas Miasojedovas
Vilnius University
16 PUBLICATIONS **161** CITATIONS
SEE PROFILE

Juozas Vidas Grazulevicius
Kaunas University of Technology
237 PUBLICATIONS **2,603** CITATIONS
SEE PROFILE

Saulius Jursenas
Vilnius University
146 PUBLICATIONS **1,115** CITATIONS
SEE PROFILE

THE JOURNAL OF PHYSICAL CHEMISTRY C

Article

pubs.acs.org/JPCC

Pyrenyl-Functionalized Fluorene and Carbazole Derivatives as Blue Light Emitters

S. Krotkus,[†] K. Kazlauskas,*[,†] A. Miasojedovas,[†] A. Gruodis,[‡] A. Tomkeviciene,[§] J. V. Grazulevicius,[§] and S. Jursenas[†]

[†]Institute of Applied Research and [‡]Department of General Physics and Spectroscopy, Vilnius University, Saulėtekio 9-III, LT-10222, Vilnius, Lithuania

[§]Department of Organic Technology, Kaunas University of Technology, Radvilėnų 19, LT-50254, Kaunas, Lithuania

Supporting Information

ABSTRACT: New pyrenyl mono- and disubstituted fluorene and carbazole derivatives were synthesized and investigated as blue-emitting materials. Most of the synthesized compounds were capable of forming glasses with glass transition temperatures up to 105 °C. The mono- and disubstituted compounds exhibited efficient emission in a diluted form with the peak wavelengths of 416 and 422 nm and quantum yields of 0.72 and 0.82, respectively. Photophysical properties of the compounds in dilute solutions and solid state were investigated experimentally and rationalized by density functional theory calculations. The calculations revealed a low energy barrier for intramolecular twisting in the ground and excited states. The electronic spectra of the compounds were dominated by an allowed "pyrene-like" $S_0 \rightarrow S_2$ transition prevailing in nearly perpendicularly twisted molecular structures and competitive $S_0 \rightarrow S_1$ transition becoming increasingly allowed for more planar conformers. The disubstituted compounds demonstrated a 3-fold enhanced oscillator strength of $S_0 \rightarrow S_1$ transition, giving rise to the enhanced fluorescence quantum yield, significant shortening of the fluorescence lifetimes (from 2.5 ns down to 1.0 ns), and 3-fold reduced amplified spontaneous emission threshold as compared with those of the monosubstituted compounds. Introduction of the bulky dihexyl group into the pyrenyl-disubstituted fluorene enabled remarkable suppression of emission concentration quenching in a solid state and ensured high emission quantum yield (0.63) in the wet-casted neat films. Pyrenyl disubstitution of fluorene and a sterically hindered aliphatic group enabled observation of a low amplified spontaneous emission threshold (20 kW/cm^2) for the compound dispersed in the inert polystyrene host at a rather large (5 wt %) chromophore concentration.

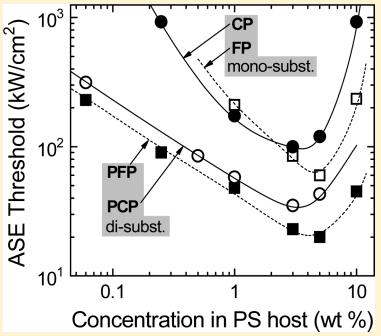

INTRODUCTION

Rapidly improving performance of organic optoelectronic devices (organic light emitting diodes (OLED), organic thin films transistors (OTFT), and organic solar cells) is mainly accounted for by rational design and synthesis of novel molecular structures demonstrating superior properties. Until now, the best light-emitting-device performance in terms of efficiency and lifetime has been achieved through the utilization of low-molecular-weight compounds.[1] Small-molecule compounds have a strictly defined structure and thus, can address specific function, deliver purity unachievable by polymers, and can be both solution-processed and sublimed in vacuum to form functional layers in a device.[2−4] Although solution-cast devices offer simplified manufacturing and are an attractive low-cost alternative, they are still struggling to match the performance of their vacuum-deposited counterparts.[5] Current progress in solution-processed small-molecule OLEDs is encouraging and shows promise to catch up shortly with the state-of-the-art evaporated devices.[3,6] Thus, a search for new small-molecule compounds with superior optical and electrical properties in addition to high glass transition temperature and a low tendency to crystallize is in demand. In this regard, multifunctional compounds consisting of several bridged polycyclic aromatic moieties are considered to be promising raw material for the state-of-the-art, solution-processable light-emitting devices.[7−9] In most cases, the multifragment compounds possess twisted conformations, which ensure glass-forming properties and have important implications on layer functional properties of a device and, thus, need to be addressed.[10,11]

Two of the most exploited aromatic units constituting the multichromophoric systems are carbazole and fluorene, which, in fact, by proper substitution are capable of delivering multifunctional properties. For instance, carbazoles, known as classic hole transporters, are also utilized as light-emitting materials.[12−15] Meanwhile, fluorenes, which are famous for high fluorescence efficiency, easy wavelength-tunability, and therefore, employed as an active media in OLEDs[16] and organic lasers,[17] have also been employed in photovoltaic devices.[18]

Functionalization of carbazole and fluorene units via substitution at the 2,7-positions have demonstrated great potential and advantage over typical 3,6-substitution (for the

Received: January 5, 2012
Revised: March 7, 2012
Published: March 8, 2012

   dx.doi.org/10.1021/jp300161k | J. Phys. Chem. C 2012, 116, 7561−7572

carbazole moiety) for light-emitting device applications by yielding extended conjugation, enhanced emission efficiency, and, in some cases, bipolar charge carrier transport with electron and hole mobilities as high as 10^{-3} $cm^2/(V\ s)$.[12,19,20] Previously hardly achievable due to inefficient synthesis routes, carbazole substitution at the 2,7-positions results in a more symmetrical, elongated molecule shape, which is beneficial for the preparation of parallel-to-a-substrate oriented molecule layers, facilitating light outcoupling from an OLED structure,[21,22] and enabling a reduction of amplified spontaneous emission threshold.[23]

Integration of the pyrene functional unit into the unified conjugated structure with the fluorene and carbazole chromophores at 2- and 2,7-positions is based on the following arguments. Pyrene moiety has long been known as a fluorescent label and probe owing to its tendency to excimer formation, long-lived excited states, high fluorescence efficiency, and sensitivity of these features to microenvironmental changes.[24] However, only recently has pyrene started to be used as an organic semiconductor for advanced applications in materials science and organic electronics. Pyrene-based, low-molecular-weight compounds and polymers have been employed as active components in OTFTs[25] and solar cells.[24] Theoretical and experimental findings have indicated that suppression of pyrene aggregation by bulky substitutents can result in high solid-state fluorescence quantum efficiencies.[26,27] Both vacuum-deposited[28,29] and solution-processed[30,31] layers of fluorene compounds substituted with pyrene at the 2- and 7-positions have been used as efficient blue emitters in OLEDs. Pyrene-modified oligocarbazoles at the 3- and 6-positions have been demonstrated to express higher fluorescence quantum efficiencies than the analogous oligomers without pyrene.[32] It is worth noting that there is a lack of reports on the carbazoles substituted with pyrenes at 2- or 2,7-positions. More recently, pyrene-cored 9,9-dialkylfluorene starbursts were utilized as an optical gain media for a low-threshold organic semiconductor laser application.[33]

To this end, a series of pyrene-functionalized, soluble 9-alkyl-carbazole and 9-alkyl-fluorene compounds have been designed, synthesized, and investigated. Aiming for high-efficiency emitting compounds, 2- and 2,7-positions of the carbazole and fluorene moieties were utilized, which, particularly in the case of the pyrenyl-disubstituted compounds, resulted in an elongated molecular shape favorable for controlling molecule orientation in layers and, consequently, for enhancing their emission efficiency. Introduction of the different alkyl chains, ethylhexyl and dixehyl, into carbazole and fluorene moieties, respectively, permitted investigation of their effect on the glass-forming and emission properties of the wet-casted films. To reveal the emission properties of the compounds, they were thoroughly studied by measuring fluorescence spectra, fluorescence quantum yields, fluorescence decay times in dilute solutions, polymer (polystyrene) matrixes at different chromophore concentrations, and wet-casted neat films. The phophysical properties of the compounds were also assessed by density functional theory (DFT). Theoretical analysis of electronic transitions was addressed by emphasizing intramolecular twisting. The advantages of the emission properties of the pyrenyl disubstituted fluorene and carbazole compounds against monosubstituted compounds were rationalized in terms of differently twisted conformers. Intermolecular coupling peculiarities were disclosed by thorough investigations of emission concentration quenching of the compounds in a solid state. The possibility of using the mono- and disubstituted compounds as efficient blue emitters as well as optical gain media for lasing applications was explored.

EXPERIMENTAL SECTION

Proton and carbon nuclear magnetic resonance (^1H and ^{13}C NMR) spectra were taken on Varrian Unity Inova (300 MHz (^1H), 75.4 MHz (^{13}C)) spectrometer. Mass (MS) spectra were obtained on a Waters ZQ (Waters, Milford, MA, USA) and Finnigan MAT 8500 (70 eV) with a MAT 112 S Varian. Elemental analysis was performed with an Exeter Analytical CE-440 Elemental. DSC measurements were carried out using a Perkin-Elmer DSC-7 series thermal analyzer at a heating rate of 10 °C/min under nitrogen flow. TGA measurements were performed on a Mettler Toledo TGA/SDTA 851^e. The melting point (m.p.) of the materials was determined using an Electrothermal Mel-Temp apparatus. Absorption spectra of the dilute THF solutions were recorded on a UV−vis−NIR spectrophotometer Lambda 950 (Perkin-Elmer). Fluorescence of the investigated compounds in dilute THF solutions, polystyrene (PS), and neat films was excited by a 365 nm wavelength light emitting diode (Nichia NSHU590-B) and measured using a back-thinned CCD spectrophotometer PMA-11 (Hamamatsu). For these measurements, the dilute solutions of the investigated compounds were prepared by dissolving them in a spectral grade tetrahydrofuran (THF) at 1×10^{-5} M concentration. The PS films with the dispersed compounds with concentrations ranging from 0.06 to 10 wt % were prepared by mixing the dissolved compounds and PS in toluene solutions at appropriate ratios and casting the solutions on quartz substrates in ambient air. The drop-casting from THF solutions (1×10^{-3} M) was also employed to prepare the neat films of the compounds.

Fluorescence quantum yields (η) of the solutions were estimated by comparing wavelength-integrated PL intensity of the compound solutions with that of the reference. Quinine sulfate in 0.1 M H_2SO_4 with $\eta = 0.53 \pm 0.023$ was used as a reference.[34] Optical densities of the reference and sample solutions were kept below 0.05 to avoid reabsorption effects. Estimated quantum yields of the compound solutions were verified using the integrated sphere method.[35] An integrating sphere (Sphere Optics) coupled to the CCD spectrometer via optical fiber was also employed to measure η of the neat and PS films. Fluorescence transients of the samples were measured using a time-correlated single photon counting system PicoHarp 300 (PicoQuant), utilizing a semiconductor diode laser (repetition rate 1 MHz, pulse duration 70 ps, emission wavelength 375 nm) as an excitation source. Amplified spontaneous emission (ASE) measurements were carried out by exciting the films with a 40-μm-wide laser stripe focused on the film surface near its edge by using a cylindrical lens (the so-called "thin-stripe" excitation geometry).[36] Frequency-tripled (355 nm) Nd^{3+}:YAG laser (EKSPLA) with a pulse duration of 5 ns and a repetition rate of 10 Hz was used as an excitation source. Excitation power density in the ASE measurements was varied by several orders of magnitude from 1 to 2000 kW/cm^2 to determine the ASE threshold.

RESULTS AND DISCUSSION

Synthesis and Characterization. The starting compounds 2-bromo-9,9-dihexylfluorene (**1**), 2,7-dibromo-9,9-dihexylfluorene (**2**), 2-bromo-9-(2-ethylhexyl)carbazole (**3**) and 2,7-

dx.doi.org/10.1021/jp300161k | J. Phys. Chem. C 2012, 116, 7561−7572

Scheme 1. Synthesis of Pyrene-Substituted Fluorene (FP, PFP) and Carbazole (CP, PCP) Compounds

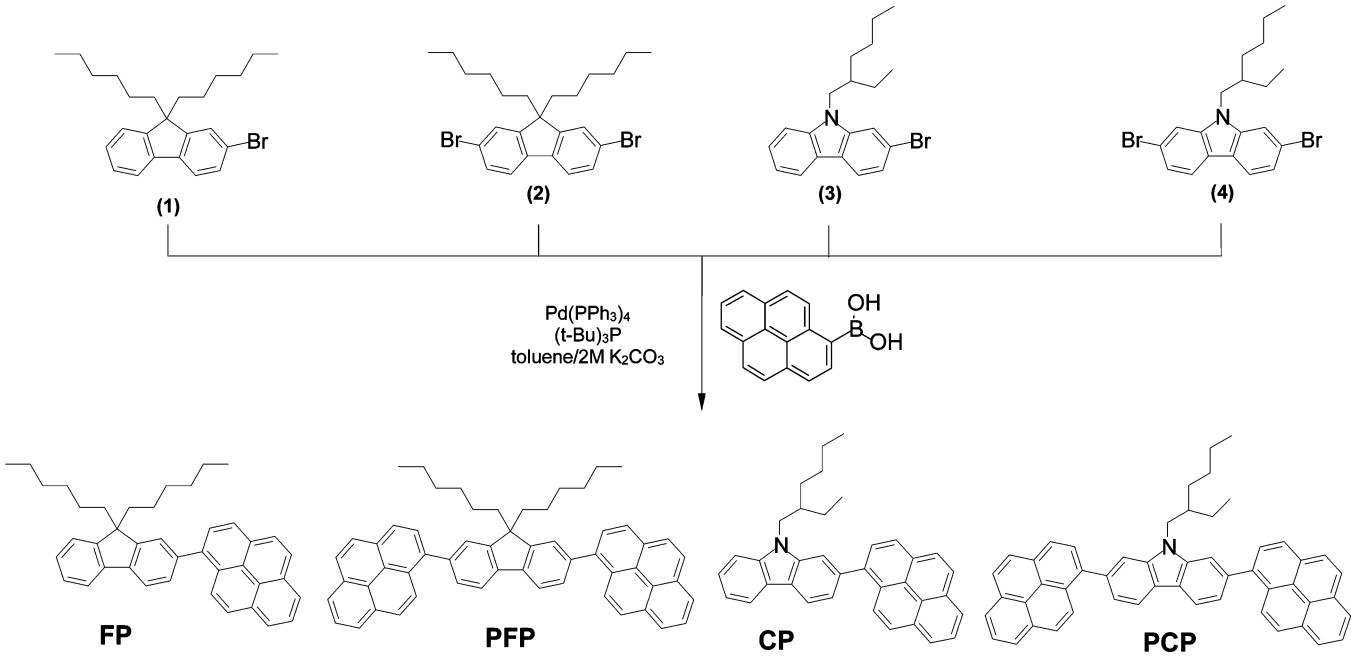

dibromo-9-(2-ethylhexyl)carbazole (**4**) were synthesized by a multistep synthetic route according to published procedures.[37−40] Pd-catalyzed Suzuki coupling reactions of bromo or dibromo compounds and pyrene-1-boronic acid were accomplished by adding a catalytic amount of bulky tri-*tert*-butylphosphine as a promoter to afford the target pyrenyl monosubstituted fluorene (FP) and carbazole (CP) compounds as well as disubstituted fluorene (PFP) and carbazole (PCP) compounds in good yields (Scheme 1). ^{1}H and ^{13}C NMR, mass spectrometry, and elemental analysis were employed to confirm the chemical structures of the above-mentioned compounds (see Synthesis Information in the Supporting Information).

Theoretical Calculations. Quantum chemical calculations of the pyrene-substituted carbazole and fluorene derivatives were performed using DFT as implemented in the Gaussian 03[41] software package. Ground-state geometries of the molecular structures were optimized at the B3LYP functional level with the 6-311G (d,p) basis set supplemented with polarization functions. Singlet transition energies, the corresponding oscillator strengths, and spatial distributions of electron density for HOMO (0, −1, −2) and LUMO (0, +1, +2) were obtained by means of the semiempirical ZINDO calculations. To simplify the calculations, long ethylhexyl and dihexyl chains of saturated hydrocarbons at fluorene (carbazole) C9 (N9) position were replaced by ethyl and diethyl groups, respectively.

The DFT calculations revealed similar electronic energy spectra, oscillator strengths, and electron density distributions for the monosubstituted FP and CP compounds up to the S_2 state. Clear differences showed up for S_3 and higher-lying states separated by more than 0.5 eV from S_1 and S_2 and, thus, might be noticeable in the absorption spectra only above 4.0 eV. Therefore, the higher-lying states will not be considered in further discussion.

To reveal the information about the states of different conformers of the singly bridged multichromophoric compounds, the optimization was performed for various dihedral angles between the neighboring units. The optimization of the total energies revealed broad energy minima of the S_0 and S_1 states with respect to the dihedral angle between the fluorene (or carbazole) and pyrene moieties (Figure 1a). Since the energies and oscillator strengths exhibited angular symmetry with respect to a 90° angle (denoting orthogonal orientation of carbazole and pyrene moieties), the parameter dependences in Figure 1 are displayed starting from this angle. On the other

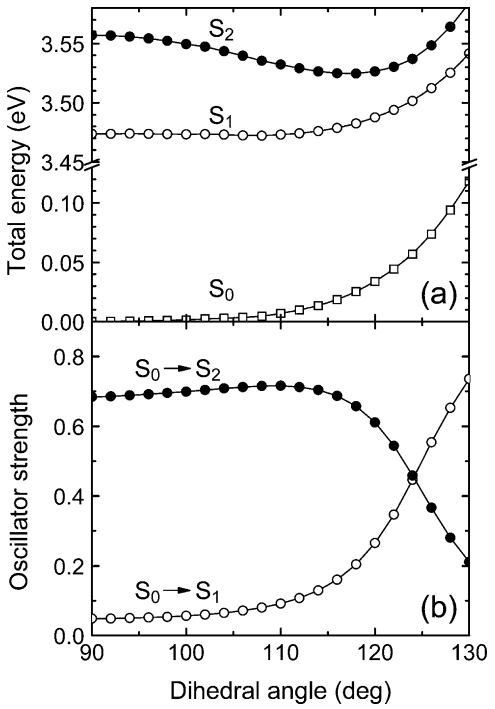

Figure 1. Calculated total energies of the ground state S_0 and the first two excited states S_1, S_2 (a) and oscillator strengths of the singlet transitions $S_0 \rightarrow S_1$, $S_0 \rightarrow S_2$ (b) as a function of the dihedral angle for the monosubstituted FP compound.

dx.doi.org/10.1021/jp300161k | J. Phys. Chem. C 2012, 116, 7561−7572

hand, for the upward transitions from S_0, the maximum accessible dihedral angle is limited by the molecule total energy, which is on the order of the thermal energy, k_BT (25 meV at room temperature). Here, k_B is the Boltzmann constant, and T is the temperature. The broad energy minimum of the monosubstituted FP and CP compounds extending over the angles of 60−120° within the k_BT implied molecules with a large variety of twist angles available in the ground state at room temperature. This also indicates weak steric effects between the fragments for the dihedral angles within this range.

An evaluation of the oscillator strengths of the two lowest transitions for this particular angle range revealed domination of the $S_0 \rightarrow S_2$ transition (Figure 1b), which is known as a "pyrene-like" transition and is polarized along the long axis of the pyrene molecule.[42] More than an order of magnitude weaker oscillator strength was obtained for the $S_0 \rightarrow S_1$ transition, which noticeably contributed only for dihedral angles above 120° or below 60°.

Interestingly, the S_2 state has shallow energy minima at 117° and 63° for the monosubstituted compounds, implying an enlarged contribution of such conformers in the excited state relaxation processes.

Electron wave function overlap for the different twist angles between fluorene (carbazole) and pyrene moieties in the monosubstituted FP (CP) compounds was visualized by calculating the HOMO and LUMO orbitals. Since in the ground state at room temperature the molecules can be twisted from the orthogonal orientation by ±30°, we present HOMO and LUMO orbitals of the monosubstituted FP compound calculated at a permissible angle of 120° (Figure 2). Calculated

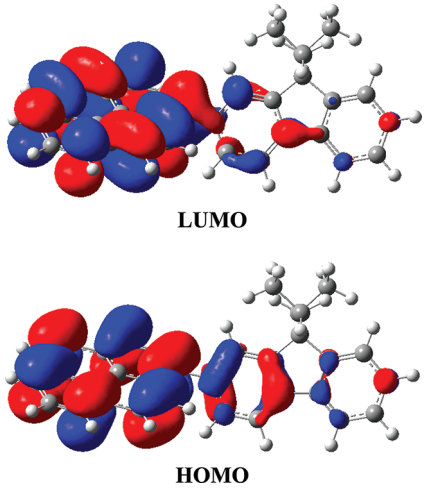

Figure 2. HOMO and LUMO of the monosubstituted FP compound calculated at a dihedral angle of 120° using the B3LYP/6-311G (d,p) basis set.

molecular orbitals indicate electron density localized predominantly on a pyrene subunit. However, nonorthogonal orientation of pyrene and fluorene subunits causes delocalization of the electron cloud toward the nearest phenyl ring of the fluorene subunit, resulting in an extended π conjugation in FP. The similar HOMO and LUMO configurations were obtained for the monosubstituted CP compound.

As in the case of the monosubstituted FP and CP compounds, disubstituted PFP and PCP compounds also expressed very similar energy spectra and oscillator strengths for the S_0, S_1, and S_2 states. In principle, the description of the monosubstituted compounds twisted at various angles in the S_0 state is also applicable to disubstituted compounds, since their total energies follow the same trend (Figure 3). The

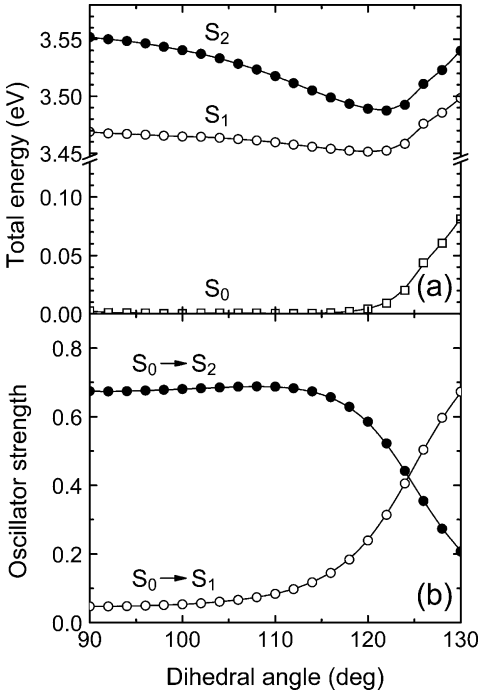

Figure 3. Calculated total energies of the ground state S_0 and the first two excited states S_1, S_2 (a) and oscillator strengths of the singlet transitions $S_0 \rightarrow S_1$, $S_0 \rightarrow S_2$ (b) as a function of dihedral angle for the disubstituted PFP compound.

disubstituted compounds, however, show an even wider angular distribution of the corresponding subunits, causing the $S_0 \rightarrow S_1$ transition to be of comparable strength to that of $S_0 \rightarrow S_2$ at large (or small) dihedral angles. Similarly to the monosubstituted compounds, the S_2 state in the disubstituted compounds also expressed energy minima with respect to the twist angle. However, the minima appeared to be slightly deeper and at the larger twist angles (122° and 58°). The revealed difference between the mono- and disubstituted compounds can be possibly experimentally detected through the intensity variations of the lowest absorption bands corresponding to these transitions.

The electron density in the HOMO and LUMO of the disubstituted PFP and PCP compounds is delocalized over the central fluorene (carbazole), and both pyrene subunits in the case that the subunits are not orthogonal (Figure 4). Since the disubstituted compounds in the ground state can possess various twist angles (60−120°) such a distribution of electron density is highly probable.

Summarizing the DFT calculation results, it is evident that both $S_0 \rightarrow S_1$ and $S_0 \rightarrow S_2$ transitions contribute to the optical spectra of fluorene and carbazole derivatives substituted with pyrene at the 2- and 2,7-positions, which is in agreement with other reports on 1-substituted pyrene compounds.[42] A novel result is the low activation energy for the intramolecular twisting of the large singly bonded chromophores, causing the enhanced contribution of the $S_0 \rightarrow S_1$ transition at the large twisting angles (above 120° or below 60°). Importantly, the disubstituted compounds display conformers with larger twist angles than those of the monosubstituted compounds and,

dx.doi.org/10.1021/jp300161k | J. Phys. Chem. C 2012, 116, 7561−7572

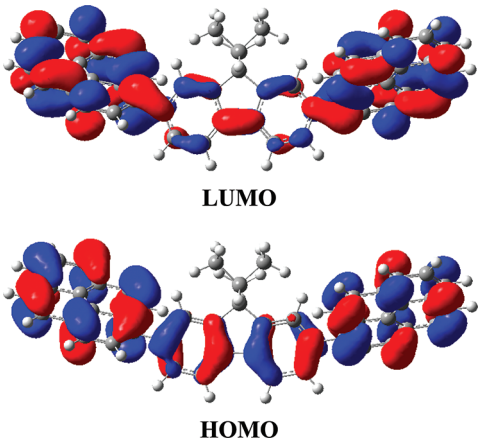

Figure 4. HOMO and LUMO of the disubstituted PFP compound calculated at a dihedral angle of 120° using the B3LYP/6-311G (d,p) basis set.

thus, greater impact of the S_1 state, which determines emission properties, the main subject of the present study.

Thermal Properties. Thermal stability and related morphology changes of pyrene-substituted fluorene and carbazole derivatives were estimated using thermogravimetric analysis (TGA) and differential scanning calorimetry (DSC), respectively. The thermal characteristics of the synthesized compounds are summarized in Table 1. The FP, CP, PFP, and

Table 1. Thermal Properties of the Pyrenyl Monosubstituted (FP, CP) and Disubstituted (PFP, PCP) Fluorene and Carbazole Compounds

	T_g[a] (°C)	T_m[a] (°C)	T_{cr}[a] (°C)	T_{ID}[b] (°C)
FP	17	89[c]		414
CP	30	136[c]		409
PFP	76	243	161	447
PCP	105	208[c]		507

[a]Determined by DSC, scan rate 10 °C/min, N_2 atmosphere. [b]5% weight loss determined by TGA, heating rate 10 °C/min, N_2 atmosphere. [c]First heating only.

PCP compounds exhibited fairly high thermal stability, with a 5% weight loss temperature (T_{ID}) over 400 °C.

The DSC measurements revealed that the CP, PFP, and PCP compounds are able to form molecular glasses at room temperature. The compounds were isolated after the synthesis as crystalline materials, and their first DSC heating scans revealed endothermal melting signals. However, no crystallization was observed during the cooling scans, which indicates a direct transition from the melt to glassy state. In the second DSC heating scans, all the compounds exhibited glass transitions with glass transition temperatures (T_g) ranging from 17 to 105 °C. The detailed thermal characteristics of the compounds are summarized in Table 1. Typical DSC thermograms for the disubstituted PCP compounds are given in Figure 5. The first DSC scan of the PCP revealed melting at 208 °C, whereas after cooling, the second heating scan revealed glass transition only at 105 °C. Similar DSC thermograms were recorded for the rest of the compounds, except the PFP. The PFP compound crystallized during the second heating scan at 161 °C and then melted at 243 °C.

The revealed thermal properties show a remarkably higher T_g for the disubstituted PFP and PCP compounds than for the

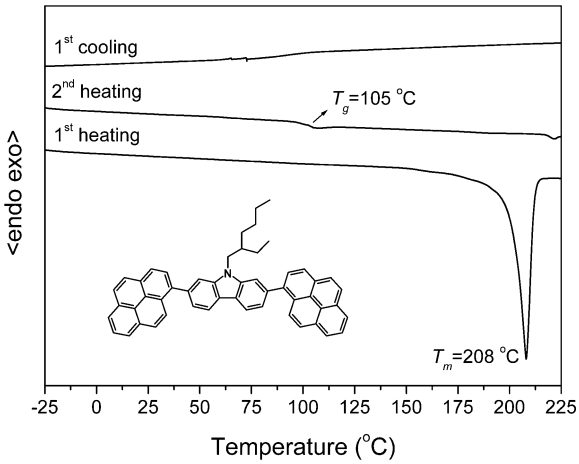

Figure 5. DSC thermograms of the disubstituted PCP compound in N_2 atmosphere at a heating/cooling rate of 10 °C/min.

monosubstituted FP and CP compounds. It is also interesting to note that pyrene-substituted carbazole derivatives CP and PCP appeared to have higher T_g values than the corresponding pyrene-substituted fluorene compounds FP and PFP. The T_g of CP (30 °C) is higher than that of FP (17 °C), and the T_g of PCP (105 °C) is higher than that of PFP (76 °C).

Absorption Spectra. The normalized absorption and fluorescence spectra of the investigated pyrene-functionalized fluorene and carbazole compounds in dilute THF solutions, dilute polystyrene (PS) matrixes, and neat films are shown in Figure 6 (see also Figure S1 in the Supporting Information). The details of the photophysical properties of the compounds are summarized in Table 2. The absorption spectra of monosubstituted FP and CP compounds are similar and feature a dominant band peaked at 347 nm and a less pronounced band at 300 nm. The absorption spectra of disubstituted PFP and PCP compounds also look similar; nevertheless, their main absorption band is significantly broadened and red-shifted (by ~10 nm) as compared with that of the monosubstituted compounds. In addition, the doubling of the number of pyrene functional units is found to nearly double the extinction coefficient, that is, double the oscillator strength of the lowest-energy transitions, which might be important for some device applications. The weaker intensity band at 300 nm, which can also be traced in the spectra of disubstituted compounds, is attributed to a local excitation of the individual carbazole and fluorene fragments, which have distinct absorption peaks in the vicinity of this energy.[13,43]

Taking into account that an onset of absorption of single fluorene,[43] carbazole,[13,44] and pyrene[28,45] units is below 340 nm, the dominant absorption band of the monosubstituted compounds (λ_{abs} = 347 nm) as well as of the disubstituted compounds ($\lambda_{abs} \approx$ 360 nm) can be assigned to a delocalized $\pi-\pi^*$ excitation of the pyrene-substituted fluorene/carbazole conjugated system, in agreement with the literature data on similar pyrene-functionalized fluorene compounds.[28] This assignment is also well-supported by our theoretical calculations (see section Theoretical Calculations, Figures 2 and 4), which indicate pyrene-centered molecular charge delocalization toward carbazole/fluorene subunits resulting in the extended π-conjugation. The significantly broadened absorption spectra of the pyrene-substituted compounds with respect to that of an unsubstituted pyrene[42] are consistent with our theoretical

dx.doi.org/10.1021/jp300161k | J. Phys. Chem. C 2012, 116, 7561−7572

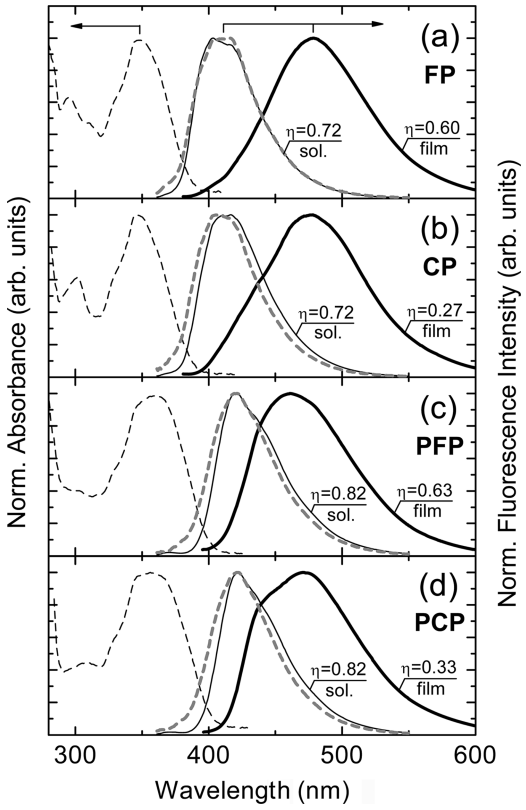

Figure 6. Absorption (dashed thin line) and fluorescence spectra of the (a) FP, (b) CP, (c) PFP, and (d) PCP compounds in 10^{-5} M THF solution (thin, solid line), polystyrene matrix at 0.06 wt % concentration (thick, dashed line), and neat films (thick solid line). Fluorescence quantum yields are indicated.

observations on a low-energy barrier for intramolecular twisting, indicating an inhomogeneous system of twisted conformers. Moreover, the broadened and red-shifted absorption band of the disubstituted PFP and PCP compounds, as compared with that of the monosubstituted FP and CP compounds, obviously implies enhanced conjugation and is consistent with the wider distribution of the allowed twist angles between the carbazole (fluorene) and pyrene units, causing the oscillator strength enhancement of the $S_0 \rightarrow S_1$ electron transition (Figure 3). The agreement between the calculated transition energies and those obtained experimentally from the absorption spectra is fairly good, even though the solvation shell effects were not included in the calculations.

Fluorescence Spectra. Excitation at 365 nm of the dilute THF solutions of the pyrenyl mono- and disubstituted fluorene/carbazole compounds resulted in a highly efficient fluorescence in the blue spectral region with bands peaked at 403−422 nm (Figure 6). As in the case of absorption spectra, the emission bands of the studied compounds were red-shifted as compared with the emission of single fluorene and carbazole moieties (λ_F^{max} < 360 nm)[44,46] as well as to that of a single pyrene moiety (λ_F^{max} < 390 nm),[42] indicating an excitation delocalization over the several moieties in the excited state. The emission bands of all the studied compounds were Stokes-shifted by approximately the same value (60 nm); however, a slightly larger bathochromic shift of the disubstituted compound emission with respect to the monosubstituted compound emission indicated an enhanced conjugation of the former. This is also in agreement with our theoretical predictions indicating the larger inhomogeneity of the intramolecularly twisted conformers and the increased role of the S_1 state.

Fluorescence quantum yields of the compounds in dilute THF solutions were determined to be 0.72 for the monosubstituted FP and CP compounds, whereas a higher value of η (0.82) was attained for the disubstituted PFP and PCP compounds (see Table 2). Slightly higher values of η obtained for the disubstituted compounds are consistent with the enhanced oscillator strength of the lowest electron transitions revealed from the absorption measurements and also with the higher degree of delocalization of electronic excitations deduced from the emission spectra. Interestingly, the choice of the carbazole or fluorene moieties as the central chromophore has no effect on the fluorescence quantum yield of the noninteracting multichromophoric compounds, confirming the electron density localizes mainly on the pyrene functional group (see Figures 2 and 4).

Fluorescence spectra of the pyrene-substituted fluorene/carbazole derivatives embedded in rigid PS matrixes at low concentrations (<0.25 wt %) were similar to the solution spectra (Figure 6). The small blue shift of the fluorescence spectra observed for the compounds dispersed in a rigid PS matrix can be attributed either to a different polarity of the surrounding medium or to a suppressed intramolecular twisting in the excited state with respect to that in the solution. The possibility of an intramolecular twisting will be further discussed in the section Intramolecular twisting in the excited state.

In contrast to the emission spectra of FP, CP, PFP, and PCP compounds in solution and the PS matrix, the spectra of their neat films are structureless, considerably red-shifted, and broadened (Figure 6). In addition, the reduction of the fluorescence quantum yield of the neat films as compared with that of the solutions from 0.72 to 0.60/0.27 for the monosubstituted FP/CP compounds and from 0.82 to 0.63/0.33 for the disubstituted PFP/PCP compounds, respectively,

Table 2. Photophysical Properties of the Dilute (10^{-5} M) THF Solutions and Neat Films of Pyrene-Functionalized Fluorene and Carbazole Compounds FP, CP, PFP, and PCP

		solution						neat film		
		λ_{abs}[a] (nm) (ε[b], L mol^{-1} cm^{-1})	λ_F^{max}[c] (nm)	η	τ (ns)	τ_R[d] (ns)	τ_{NR}[d] (ns)	λ_F^{max}[c] (nm)	η	τ (ns)
mono-	FP	347 (37360), 296 (23840)	403, 416	0.72	2.8	3.8	9.8	478	0.60	2.3 (94%), 13.0 (6%)
	CP	347 (37540), 302 (23150)	410, 416	0.72	2.3	3.2	8.1	478	0.27	2.8 (42%), 13.2 (58%)
di-	PFP	360 (69900)	422	0.82	1.0	1.2	5.6	461	0.63	0.9 (77%), 6.0 (23%)
	PCP	357 (58590)	422	0.82	1.0	1.2	5.6	470	0.33	1.1 (52%), 5.0 (48%)

[a]Peak wavelength of absorption bands. [b]Molar extinction coefficient. [c]Wavelength at fluorescence band maximum. [d]Radiative and nonradiative decay time constants calculated as τ/η and $\tau/(1-\eta)$, respectively.

dx.doi.org/10.1021/jp300161k | J. Phys. Chem. C 2012, 116, 7561−7572

was observed. These features clearly evidence the emission originating from excimer states formed as a result of molecule aggregation in the solid state.

Since pyrene is known to readily form excimers at high chromophore concentrations with an excimer-related fluorescence band at ~485 nm,[47−49] the featureless broad emission band observed for the neat films of the mono- and disubstituted compounds (at 461−478 nm) can be naturally associated with pyrene excimers. The more red-shifted and slightly broader spectral bands of the monosubstituted compounds as compared with those of the disubstituted compounds can be explained assuming a less complex three-dimensional conformation of the former, enabling tighter molecular arrangements (aggregation) and, thus, stronger interaction of adjacent pyrene moieties, resulting in a more pronounced excimer formation in the solid state.

It is worth noticing that the neat films of FP and PFP bearing a dihexyl chain at the fluorene C9 position exhibited relatively high quantum efficiencies of ~0.6, whereas 2-fold smaller efficiencies were obtained for the films of CP and CPC compounds with an ethylhexyl chain at the carbazole N9 position. The fluorescence quantum yields of ~0.6 are rather high for the unencapsulated neat films wet-casted under ambient air conditions. The 2-fold smaller η is caused by the more effective fluorescence quenching due to enhanced aggregation in CP and CPC containing a single ethylhexyl chain. Meanwhile, FP and PFP featuring dihexyl substitutents effectively suppress aggregation and, thus, in larger part can avoid aggregation-induced emission quenching. This result implies the compounds with a dihexyl chain are more favorable for application as active layers in light-emitting devices than those with an ethylhexyl chain.

Fluorescence Decay Dynamics. To get insight into excited state relaxation processes of the pyrenyl-functionalized fluorene/carbazole compounds and to determine the governing relaxation pathway, fluorescence transients of FP, CP, PFP, and PCP were investigated. The transients measured at the fluorescence band maxima of the studied derivatives in the dilute solutions and the neat films are presented in Figure 7. Excited state relaxation of the compounds in a solution was found to follow a single exponential decay profile with estimated fluorescence lifetimes (τ) of 2.3−2.8 ns for the monosubstituted compounds and more than 2-fold shorter ones (1.0 ns) for the disubstituted compounds. The estimated lifetimes are 2 orders of magnitude shorter than that of the unsubstituted pyrene, indicating the allowedness of the lowest $S_1 \rightarrow S_0$ transition. This agrees with the shortened lifetime (down to 2−3 ns) obtained for other 1-pyrene substituted derivatives.[42] Moreover, the 2.5-fold shortening of the lifetime (down to 1 ns) accompanied by an increased fluorescence quantum yield from 0.72 to 0.82 in solution for the disubstituted compounds as compared with those for the monosubstituted compounds shows the $S_1 \rightarrow S_0$ transition to be the dominant. This is in agreement with the larger calculated intramolecular twisting angle of the disubstituted compounds with significantly higher $S_0 \rightarrow S_1$ oscillator strength.

The increase in the electron delocalization in the disubstituted compounds due to their less twisted conformers is accompanied by an enlarged oscillator strength and, consequently, transition dipole moment, which should cause a larger radiative decay rate (k_R). To evaluate the contributions of radiative and nonradiative decay processes in the studied compounds, radiative and nonradiative decay time constants, τ_R and τ_{NR}, respectively, were estimated (see Table 2). The calculated τ_R values for the disubstituted PFP and PCP compounds amounting to 1.2 ns is found to be nearly 3 times shorter (implying nearly 3-fold larger oscillator strength of the $S_1 \rightarrow S_0$ transition) than those deduced for the monosubstituted FP and CP compounds, 3.8 and 3.2 ns, respectively. To compare, variation of τ_{NR} between the mono- and disubstituted compounds amounted to less than 50%, unambiguously indicating the governing role of radiative decay processes in the compound dilute solutions.

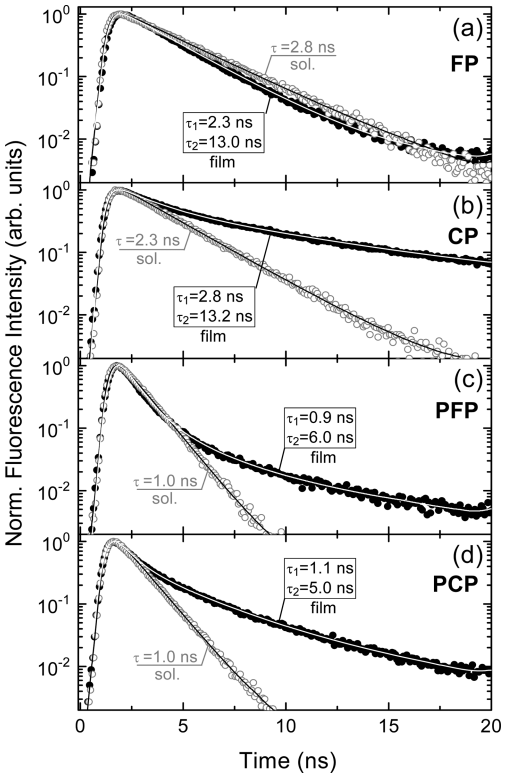

Figure 7. Fluorescence transients of the 10^{-5} M THF solutions (open circles) and neat films (solid points) of (a) FP, (b) CP, (c) PFP, and (d) PCP measured at the fluorescence band maxima. Lines indicate single or double exponential fits to the experimental data. Fluorescence lifetimes (τ) are indicated.

The fluorescence transients of the neat films clearly exhibit nonexponential behavior, pointing out several different origins of the radiative transitions. The transients were fairly well described by using a double exponential decay model yielding two decay components with different fractional intensities, that is, different contributions to the overall decay profile (see Table 2). Reduced χ^2 values, which were used together with weighted residuals as the goodness-of-fit criteria, did not exceed 1.5, ensuring a reliable description of the experimental data.

The fast decay component (τ_1) of the neat films varied from ~1 ns for the disubstituted compounds to ~2.5 ns for the monosubstituted compounds. This component had a dominant contribution (fractional intensity 77−94%) in the fluorescence decay dynamics of FP and PFP, but it contributed roughly equally (fractional intensity 42−52%) as the slow component (τ_2) to the excited state relaxation in the case of CP and PCP. The fast component is attributed to exciton migration, and the migration-induced exciton quenching. Bearing in mind the formation of molecular aggregates in the neat films of the monosubstituted compounds as well as of the disubstituted

dx.doi.org/10.1021/jp300161k | J. Phys. Chem. C 2012, 116, 7561−7572

compounds, as evidenced from their excimer fluorescence band, the slow relaxation component (with τ_2 varying from ~5 ns in the disubstituted compounds to ~13 ns in the monosubstituted compounds) can be attributed to the aggregated states. The prevalence of the fast relaxation in FP and PFP over excimer-like fluorescence decay significantly contributing in the CP and PCP compounds can be justified by the different types of alkyl chains attached to the central fluorene C9 and carbazole N9 positions, resulting in different molecular packing. Obviously, the dihexyl substituent in FP and PFP causes more pronounced steric hindrance effects and, thus, is more favorable for preventing molecule agglomeration in the solid state than the less bulky ethylhexyl substituent in the CP and PCP.

Intramolecular Twisting in the Excited State. Intramolecular twisting of singly bonded sterically hindered groups is a frequently observed phenomenon for multifragment compounds.[10] Excited state decay transients of the compounds molecularly dispersed in PS host at concentrations ranging from 1 to 10 wt % were measured and reliably described by a double exponential decay model with the dominant decay component having a fractional intensity of over 83% (see Figure S3 and Table S1 in the Supporting Information). The estimated dominant lifetimes (τ) for the compounds in the PS matrix at low chromophore concentration were found to be 30% longer than those obtained for the dilute solutions (Figure 8b, Table S1 in the Supporting Information). This provides an additional prove of the intramolecular twisting in the excited state.

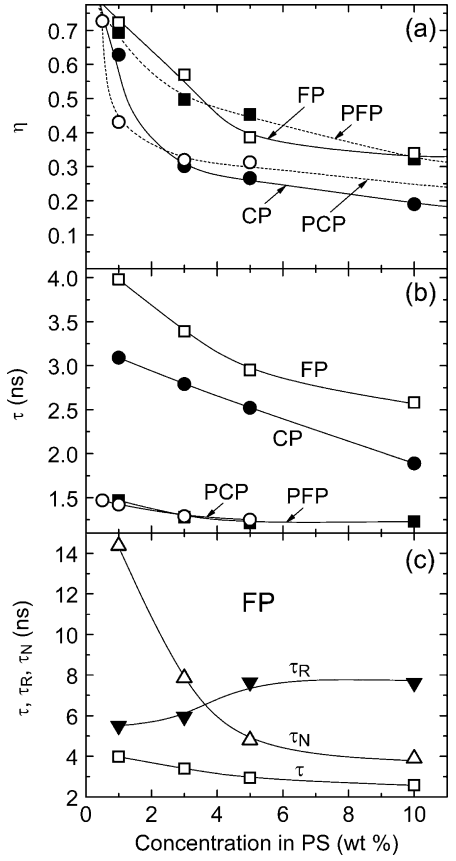

Figure 8. (a) Fluorescence quantum yield and (b) dominant lifetime of FP, CP, PFP, and PCP as a function of chromophore concentration in polystyrene matrix. (c) Fluorescence decay time (τ) as well as calculated radiative (τ_R) and nonradiative (τ_N) decay time of the FP vs the compound concentration in a PS matrix. Lines are guides for the eye.

The DFT calculations show potential energy minima in the excited states of the monosubstituted compounds and, in particular, of the disubstituted compounds in the vicinity of a 120° (60°) twist angle (Figure 1a and Figure 3a). Possibly, the minima could be more pronounced if the solvation-shell effects were included in the calculations. Since the ground state has the flat potential minimum allowing for a wide distribution of the twist angles, excitation creates differently twisted conformers. In a solution, the excitation migrates to the potential minimum, resulting in 120° twisted conformers and yielding remarkable shortening of the excited state decay time (down to 1 ns for the disubstituted compounds). Whereas in a rigid PS matrix, the intramolecular twisting is restricted, implying smaller average twist angle causing emission from the differently twisted conformers and resulting in the observed emission blue shift, nonexponential decay and enhanced average decay time.

Fluorescence Concentration Quenching. Emission quenching followed by increasing chromophore concentration is a serious issue limiting utilization of highly emissive compounds in an undiluted form and, thus, hampering their applicability in solid-state light-emitting devices. The issue has been addressed by many authors and successfully approached by designing complex (e.g., spiro-, starburst-, or dendrimer-like) three-dimensional molecular structures or employing additional pendant groups (e.g., branched aliphatic chains) inhibiting molecule agglomeration and, consequently, concentration quenching.[27,50−52] From this point of view, it is of interest to explore the concentration quenching effects in our blue-emitting pyrene-functionalized fluorene/carbazole compounds. Fluorescence quantum efficiency measurements of FP, CP, PFP, and PCP performed in the dilute solutions and the neat films revealed a 20−60% efficiency drop for the films, which was accounted for by the molecule agglomeration. The variation in the efficiency drop to a larger extent was caused by the different pendant alkyl groups, resulting in the minimal drop (~20%) and, therefore, suppressed aggregation for the compounds having more bulky dihexyl group (see Table 2).

Concentration quenching in our compounds was explored by dispersing them in a rigid transparent polystyrene host and estimating fluorescence quantum efficiency changes versus concentration in the range of 0.06−10 wt % (Figure 8a). To get a more complete picture, quantum yield data were supplemented by excited state decay times measured at the different chromophore concentrations (Figure 8b). At low chromophore concentration (≤1 wt %), η values approached those of noninteracting molecules of the studied compounds in dilute solutions. Increasing the chromophore concentration up to 10 wt % caused a remarkable emission quantum efficiency drop down to 0.2−0.25 for CP and PCP and down to 0.35 for FP and PFP. As in the case of the neat films, a smaller efficiency drop and, thus, weaker concentration quenching was experienced by pyrene-subsituted compounds bearing dihexyl substitutents, which in contrast to ethylhexyl chain was more beneficial in preventing molecular aggregation. However, it is noteworthy that molecule agglomeration in the PS films is of a different nature from that observed in the neat films, since no band-broadening or pronounced red shift attributed to excimer emission were observed in the fluorescence spectra of the PS films up to 10 wt % concentration (see Figure S2 in Supporting Information).

dx.doi.org/10.1021/jp300161k | J. Phys. Chem. C 2012, 116, 7561−7572

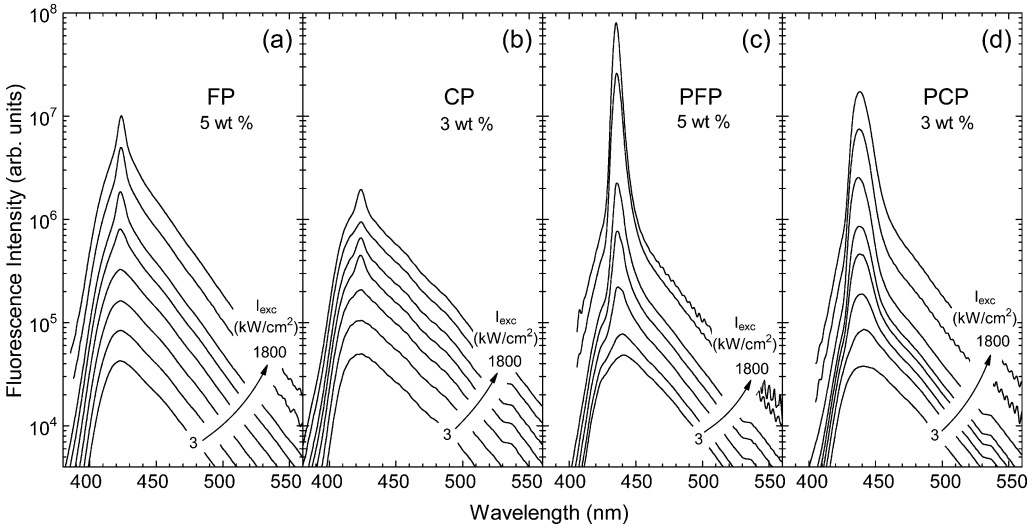

Figure 9. Excitation power dependence of the edge emission spectra of (a) FP, (b) CP, (c) PFP, and (d) PCP molecularly dispersed in PS matrix at optimal concentration (indicated).

The different molecule packing is also confirmed by lower η values of the molecularly doped PS films at high chromophore concentrations with respect to those of the neat films. The results obtained by the other authors and our data indicate that fluorescence quenching in pyrene-functionalized compounds occurs as a result of π-stacking of the planar pyrene moieties, which in FP, CP, PFP, and PCP are much less protected against aggregation than they are, for example, in pyrene-cored dendrimers or starburst compounds.[33,51,52]

The estimated dominant lifetimes of the compounds in PS matrix with the increasing chromophore concentration is depicted in Figure 8b. At the lowest concentration, the lifetimes are determined by molecular properties. As in the case of dilute solutions, the obtained τ of the disubstituted compounds was ~2-fold shorter than those of the monosubstituted compounds. An increase in the chromophore concentration in the PS matrix was accompanied by a monotonic lifetime shortening, which was more rapid for the monosubstituted compounds than for the disubstituted compounds. The decrease in τ with an increase in the concentration from 1 to 10 wt % for the monosubstituted compounds amounted to 1.6 times, as compared with 1.2 times for the disubstituted compounds.

The deduced radiative and nonradiative decay time constants for one of the compounds (FP) are depicted in Figure 8c. Taking into account the relationship $1/\tau = 1/\tau_R + 1/\tau_N$, it is apparent that the tendency of τ shortening vs concentration is governed by continuously decreasing τ_N, which follows the same trend as τ. On the contrary, τ_R exhibited a slow increase with concentration. The similar behaviors signifying nonradiative deactivation as the dominant excited state relaxation pathway were also obtained for the rest of the pyrene-functionalized fluorene and carbazole compounds. The enhanced nonradiative decay channel observed with increasing concentration can be justified by the increased intermolecular coupling of exciton transition dipole moments promoting excitation migration via a hopping process to low energy quenching sites (defects, distortions etc.) The prevalence of nonradiative decay processes of the compounds experiencing concentration quenching in a polymer matrix opposes the dominant role of radiative decay, which manifests upon the molecule condensation into the neat solid films. Obviously, this is determined by the distinct molecule packing in the neat films and formation of emissive excimer states, which preserve relatively high (up to 0.63) fluorescence quantum efficiency and are responsible for the long-lived excited states.

Amplified Spontaneous Emission. To reveal the intrinsic material potential for light amplification, the pyrene-functionalized fluorene and carbazole compounds FP, CP, PFP, and PCP were examined without utilization of external resonators or patterned distributed feedback grating structures. The simplest and, nevertheless, the most appropriate technique by far used to compare the performance of different materials for lasing application excluding effects of resonant cavity is based on ASE measurements.[53,54] The technique is based on an excitation of slab waveguide samples with a pulsed laser stripe and registration of an edge emission spectrum from a sample.[36,55,56] Essentially, spontaneous emission of the material traveling along the excitation path is enhanced by the stimulated transitions, thus resulting in the spectral narrowing of the emission at a certain pump intensity, that is, ASE threshold intensity (I_{ASE}^{th}). The application of a photopumping in the ASE measurements is beneficial in that the amplified emission can be studied without complications associated with current injection, charge transport, electrodes, etc.

ASE properties of the compounds were investigated in a PS matrix at various chromophore concentrations to elucidate the influence of molecular structure-determined intermolecular coupling on the ASE performance. The preference for the PS matrix was based on the better ASE performance achieved for conjugated compounds in this matrix as compared with that observed in the other polymer matrixes, such us poly(methylmethacrylate), poly(vinyl butyral), poly(*N*-vinyl carbazole), and poly(methyl phenylsilane).[57]

Figure 9 depicts excitation power dynamics of the edge emission spectra of the FP, CP, PFP, and PCP molecularly dispersed in the PS. The dynamics is presented for the optimal (3−5 wt %) chromophore concentration, for which I_{ASE}^{th} attains a minimal value. At the lowest excitation power density, all the compounds demonstrate a broad, spontaneous emission band, which is bathochromically shifted by a few tens of nanometers due to a reabsorption effect. The effect is also responsible for

dx.doi.org/10.1021/jp300161k | J. Phys. Chem. C 2012, 116, 7561−7572

the more abrupt short-wavelength slope of the edge emission spectra as compared with that of the spectra measured in the usual backscattering configuration (see Figure 6). An increase in the pump intensity at a certain point results in the emission band narrowing, indicating an onset of ASE. The ASE peak emerges at the spontaneous emission band maximum and is located at 424 nm for the monosubstituted compounds and ~436 nm for the disubstituted compounds. The sudden emission band narrowing with the increasing pump is followed by an abrupt change in the emission intensity from linear to superlinear with the turning point at I^{th}_{ASE}. The typical spectral line width and emission intensity dependences on the excitation power density (for the disubstituted PCP compound) are displayed in Figure 10. Similar dependences were also obtained

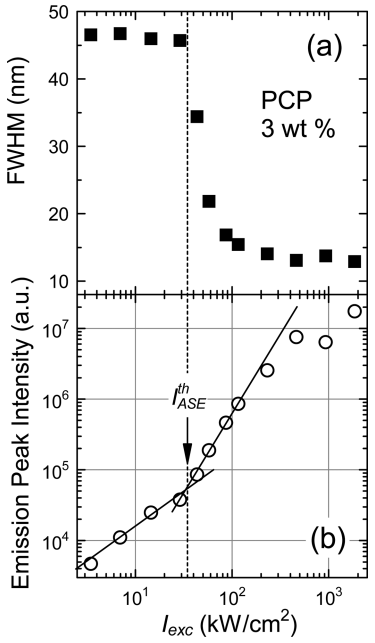

Figure 10. (a) Full width at half-maximum and (b) emission peak intensity as a function of excitation power density (I_{exc}) for the PCP compound dispersed in PS matrix at 3 wt % concentration. Lines are guides for the eye.

for the rest of the compounds (see Figure S4 in the Supporting Information). Nearly 4-fold line width narrowing and I^{th}_{ASE} of 35 kW/cm^2 were observed for PCP. The details of the ASE properties for all the studied pyrene-functionalized fluorene and carbazole compounds are summarized in Table 3.

Table 3. ASE Properties of the Pyrene-Functionalized Fluorene and Carbazole Compounds FP, CP, PFP and PCP Molecularly Dispersed in PS Matrix at the Optimal Concentration

	c_{opt}[a] (wt %)	λ_{ASE}[b] (nm)	I^{th}_{ASE} (kW/cm^2)	fwhm[c] (nm)	k_R[d] × 10^8 (s^{-1})
FP	5	424	60	9	1.7
CP	3	424	100	19	1.1
PFP	5	435	20	5	3.8
PCP	3	437	35	13	2.5

[a]Optimal concentration for which I^{th}_{ASE} is the lowest. [b]ASE peak wavelength. [c]Minimal full width at half-maximum of the ASE band. [d]Radiative decay rate.

I^{th}_{ASE} is a key parameter describing the feasibility of the material to be employed in lasing systems as an active medium. The lower I^{th}_{ASE} materials will benefit from a lower operating current density, which is critical for the device formation.[53,54] Molecule arrangement is known to play a crucial role in obtaining high fluorescence quantum efficiency and stimulated emission in a solid state; therefore, the detailed investigations of the ASE performance as a function of the concentration of the active material is of great importance. Moreover, these investigations are indispensable for determination of the optimal chromophore concentration for laser operation.[56,58]

Concentration dependencies of I^{th}_{ASE} for FP, CP, PFP, and PCP molecularly dispersed in PS matrix are illustrated in Figure 11. All the compounds demonstrate rather sensitive ASE

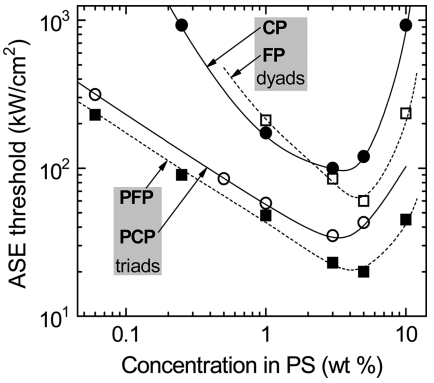

Figure 11. ASE threshold as a function of FP (open squares), CP (solid circles), PFP (solid squares), and PCP (open circles) concentration in a PS matrix. Lines are guides for the eye.

performance with respect to the chromophore concentration. At low concentration, I^{th}_{ASE} decreases, whereas at higher concentration, it increases, implying some optimal chromophore concentration for which I^{th}_{ASE} is the lowest. Since the noninteracting molecules of pyrene-functionalized fluorene and carbazole compounds exhibit higher fluorescence quantum efficiencies as compared with those of their solids and molecularly doped PS with chromophore concentration above 1 wt % (see Figure 8a), the ASE occurs for the single molecule states. An increase in the chromophore concentration (up to 3−5 wt % for our compounds) reduces the intermolecular distance and thus diminishes optical losses, lowering the I^{th}_{ASE}. However, a further increase in the concentration causes molecule agglomeration to play a decisive role, resulting in the aggregation-induced absorption in the spectral region of the amplified emission. This, consequently, enlarges optical losses and rapidly increases I^{th}_{ASE} (Figure 11).

In accordance with Einstein's B coefficient for stimulated transitions $B \propto (c^3/8\pi h\nu_0{}^3)k_R$, which is inversely proportional to the I^{th}_{ASE}. The lowest ASE threshold implies the highest radiative decay rate k_R ($k_R = \eta/\tau$). Here, c is the velocity of light, ν_0 is the frequency of light, and h is Planck's constant. This allows us to rate the compounds according to their k_R value, expecting the best ASE performance with the lowest ASE threshold to be demonstrated by the compounds featuring the highest k_R.[23] The calculated k_R's for FP, CP, PFP, and PCP molecularly dispersed in a PS matrix at optimal concentration are presented in Table 3. Indeed, as predicted from k_R estimations, PFP featuring the highest k_R (3.8 × 10^8 s^{-1}) demonstrates the lowest I^{th}_{ASE} (20 kW/cm^2), whereas CP

dx.doi.org/10.1021/jp300161k | J. Phys. Chem. C 2012, 116, 7561−7572

expressing the lowest k_R (1.1×10^8 s^{-1}) shows the highest I_{ASE}^{th} (100 kW/cm^2). The obtained lowest I_{ASE}^{th} of the pyrene-functionalized fluorene and carbazole derivatives compare well with the ASE threshold values of other classes of small molecule compounds[59] and also with the best ASE threshold values (15−20 kW/cm^2) achieved for 100% emissive perylene derivatives measured under analogous conditions with the compounds dispersed in the inert polymer host.[56,58]

Importantly, the disubstituted PFP and PCP compounds exhibit lower ASE thresholds than the monosubstituted FP and CP compounds, which again can be understood via more complex three-dimensional conformations of the disubstituted compounds obstructing closer molecule packing and, thus, diminishing intermolecular coupling and nonradiative decay processes. On the other hand, FP and PFP bearing a bulky dihexyl substituent at the fluorene C9 position exhibit lower I_{ASE}^{th} than CP and CPC containing a less bulky ethylhexyl chain at the carbazole N9 position, which is also a consequence of suppressed intermolecular coupling. These ASE results are consistent with the fluorescence spectral and concentration quenching data and suggest that multichromophoric compounds with the larger number of highly emissive singly bonded chromophores, owing to their higher emission quantum efficiencies, shorter fluorescence lifetimes, and more pronounced steric hindrance effects, are more favorable for application in light-emitting device active layers. Incorporation of optically inactive bulky aliphatic groups into the compounds is advantageous, in particular, for solution-processed thin film layers in which they prevent detrimental molecule aggregation.

CONCLUSIONS

A series of new fluorene and carbazole derivatives substituted with pyrene at 2- and 2,7-positions and expressing glass transition temperatures up to 105 °C were synthesized and investigated as promising blue light emitters. The compounds possessing two pyrenyl groups exhibited significantly higher glass transition temperatures than those having one pyrenyl group, implying an enhanced morphological stability of the disubstituted compound amorphous films for the devices. The DFT calculations indicate that the mono- and disubstituted compounds likely form twisted conformers, which facilitate formation of the glassy state.

Analysis of the electronic spectra shows that the substitution of the fluorene and carbazole compounds with pyrene results in manifestation of a "pyrene-like" $S_0 \rightarrow S_2$ transition and a partially allowed $S_0 \rightarrow S_1$ transition. The $S_0 \rightarrow S_1$ transition is enhanced at large intramolecular twisting angles, which are accessible as a result of the low activation barrier of the twisting. Importantly, the disubstituted compounds display a wider distribution of the allowed twist angles between the carbazole (fluorene) and pyrene units, implying 3-fold enhancement of the oscillator strength of the $S_0 \rightarrow S_1$ transition, causing higher fluorescence quantum efficiencies ($\eta = 0.82$) and twice as short fluorescence lifetimes ($\tau = 1.0$ ns) as compared with those ($\eta = 0.72$, $\tau \approx 2.5$ ns) for the monosubstituted compounds. Interestingly, a choice of the carbazole or fluorene moieties as the central chromophore had no effect on the fluorescence quantum yield of the noninteracting multichromophoric compounds, confirming the electron density to be mainly localized on the pyrene functional group.

A comparison of the spectral properties and excited state decay dynamics in the solution and solid state suggest an excited state twisting reaction in the solution, which is also supported by the energy potential profile revealed in DFT calculations. The concentration quenching studies performed in the solid state revealed that detrimental intermolecular coupling is diminished via introduction of bulky dihexyl groups. The sterically hindered groups allowed significant reduction of the concentration quenching and achievement of a high emission efficiency (η up to 0.63) in the unencapsulated neat films.

In accordance with a 3-fold enhancement of the radiative decay rate, 3-fold lower ASE threshold values were achieved for the disubstituted fluorene and carbazole compounds. The best ASE performance with the lowest ASE threshold (down to 20 kW/cm^2) was demonstrated by the pyrenyl-disubstituted fluorene and carbazole compounds dispersed in the inert polystyrene matrix at a rather large optimal (3−5 wt %) chromophore concentration. The results demonstrate a potential of the pyrene-functionalized fluorenes and carbazoles via their 2,7-positions as efficient blue emitters and active media for lasing applications.

ASSOCIATED CONTENT

Supporting Information

Synthesis information; absorption spectra of the neat films of FP, CP, PFP, PCP compounds; fluorescence spectra; transients; excited state decay time constants and ASE parameters of the compounds in polystyrene host at different chromophore concentrations. This material is available free of charge via the Internet at http://pubs.acs.org.

AUTHOR INFORMATION

Corresponding Author

*Phone: +370 5 2366032. Fax: +370 5 2366059. E-mail: karolis.kazlauskas@ff.vu.lt.

Notes

The authors declare no competing financial interest.

ACKNOWLEDGMENTS

The research was funded in part by a grant (No. MIP-91/2011) from the Research Council of Lithuania.

REFERENCES

(1) Reineke, S.; Lindner, F.; Schwartz, G.; Seidler, N.; Walzer, K.; Lüssem, B.; Leo, K. *Nature* **2009**, *459*, 234−238.
(2) Shirota, Y. *J. Mater. Chem.* **2005**, *15*, 75−93.
(3) Duan, L.; Hou, L.; Lee, T.-W.; Qiao, J.; Zhang, D.; Dong, G.; Wang, L.; Qiu, Y. *J. Mater. Chem.* **2010**, *20*, 6392−6407.
(4) Fisher, A. L.; Linton, K. E.; Kamtekar, K. T.; Pearson, C.; Bryce, M. R.; Petty, M. C. *Chem. Mater.* **2011**, *23*, 1640−1642.
(5) Lee, T.; Noh, T.; Shin, H.; Kwon, O.; Park, J.; Choi, B.; Kim, M.; Shin, D. W.; Kim, Y. *Adv. Funct. Mater.* **2009**, *19*, 1625−1630.
(6) Gather, M. C.; Köhnen, A.; Meerholz, K. *Adv. Mater.* **2011**, *23*, 233−248.
(7) Malinauskas, T.; Stumbraite, J.; Getautis, V.; Gaidelis, V.; Jankauskas, V.; Juska, G.; Arlauskas, K.; Kazlauskas, K. *Dyes Pigm.* **2009**, *81*, 131−136.
(8) Arbačiauskienė, E.; Kazlauskas, K.; Miasojedovas, A.; Juršėnas, S.; Jankauskas, V.; Holzer, W.; Getautis, V.; Šačkus, A. *Synth. Met.* **2010**, *160*, 490−498.
(9) Malinauskas, T.; Daskeviciene, M.; Kazlauskas, K.; Su, H.-C.; Grazulevicius, J. V.; Jursenas, S.; Wu, C.-C.; Getautis, V. *Tetrahedron* **2011**, *67*, 1852−1861.
(10) Grabowski, Z. R.; Rotkiewicz, K.; Rettig, W. *Chem. Rev.* **2003**, *103*, 3899−4032.

(11) Karpicz, R.; Puzinas, S.; Krotkus, S.; Kazlauskas, K.; Jursenas, S.; Grazulevicius, J. V.; Grigalevicius, S.; Gulbinas, V. *J. Chem. Phys.* **2011**, *134*, 204508−204516.
(12) Tomkeviciene, A.; Grazulevicius, J. V.; Kazlauskas, K.; Gruodis, A.; Jursenas, S.; Ke, T.-H.; Wu, C.-C. *J. Phys. Chem. C* **2011**, *115*, 4887−4897.
(13) Simokaitiene, J.; Grigalevicius, S.; Grazulevicius, J. V.; Rutkaite, R.; Kazlauskas, K.; Jursenas, S.; Jankauskas, V.; Sidaravicius, J. *J. Optoelectron. Adv. Mater.* **2006**, *8*, 876−882.
(14) Tao, Y.-M.; Li, H.-Y.; Xu, Q.-L.; Zhu, Y.-C.; Kang, L.-C.; Zheng, Y.-X.; Zuo, J.-L.; You, X.-Z. *Synth. Met.* **2011**, *161*, 718−723.
(15) Cho, I.; Kim, S. H.; Kim, J. H.; Park, S.; Park, S. Y. *J. Mater. Chem.* **2012**, *22*, 123−129.
(16) Yap, B. K.; Xia, R.; Campoy-Quiles, M.; Stavrinou, P. N.; Bradley, D. D. C. *Nat. Mater.* **2008**, *7*, 376−380.
(17) Komino, T.; Nomura, H.; Yahiro, M.; Endo, K.; Adachi, C. *J. Phys. Chem. C* **2011**, *115*, 19890−19896.
(18) McNeill, C. R.; Halls, J. J. M.; Wilson, R.; Whiting, G. L.; Berkebile, S.; Ramsey, M. G.; Friend, R. H.; Greenham, N. C. *Adv. Funct. Mater.* **2008**, *18*, 2309−2321.
(19) Morin, J.-F.; Beaupré, S.; Leclerc, M.; Lévesque, I.; D'Iorio, M. *Appl. Phys. Lett.* **2002**, *80*, 341−343.
(20) Shen, J.-Y.; Yang, X.-L.; Huang, T.-H.; Lin, J. T.; Ke, T.-H.; Chen, L.-Y.; Wu, C.-C.; Yeh, M.-C. P. *Adv. Funct. Mater.* **2007**, *17*, 983−995.
(21) Kim, J.-S.; Ho, P. K. H.; Greenham, N. C.; Friend, R. H. *J. Appl. Phys.* **2000**, *88*, 1073−1081.
(22) Yokoyama, D.; Sakaguchi, A.; Suzuki, M.; Adachi, C. *Org. Electron.* **2009**, *10*, 127−137.
(23) Aimono, T.; Kawamura, Y.; Goushi, K.; Yamamoto, H.; Sasabe, H.; Adachi, C. *Appl. Phys. Lett.* **2005**, *86*, 071110−071112.
(24) Figueira-Duarte, T. M.; Müllen, K. *Chem. Rev.* **2011**, *111*, 7260−7314.
(25) Bisri, S. Z.; Takahashi, T.; Takenobu, T.; Yahiro, M.; Adachi, C.; Iwasa, Y. *Jpn. J. Appl. Phys.* **2007**, *46*, L596−L598.
(26) Park, Y. H.; Rho, H. H.; Park, N. G.; Kim, Y. S. *Curr. Appl. Phys.* **2006**, *6*, 691−694.
(27) Figueira-Duarte, T. M.; Del Rosso, P. G.; Trattnig, R.; Sax, S.; List, E. J. W.; Müllen, K. *Adv. Mater.* **2010**, *22*, 990−993.
(28) Tang, C.; Liu, F.; Xia, Y.-J.; Xie, L.-H.; Wei, A.; Li, S.-B.; Fan, Q.-L.; Huang, W. *J. Mater. Chem.* **2006**, *16*, 4074−4080.
(29) Wang, Z.; Xu, C.; Wang, W.; Fu, W.; Niu, L.; Ji, B. *Solid-State Electron.* **2010**, *54*, 524−526.
(30) Walker, B.; Tamayo, A.; Yang, J.; Brzezinski, J. Z.; Nguyen, T.-Q. *Appl. Phys. Lett.* **2008**, *93*, 063302−063304.
(31) Liu, F.; Tang, C.; Chen, Q.-Q.; Shi, F.-F.; Wu, H.-B.; Xie, L.-H.; Peng, B.; Wei, W.; Cao, Y.; Huang, W. *J. Phys. Chem. C* **2009**, *113*, 4641−4647.
(32) Zhao, Z.; Xu, X.; Wang, H.; Lu, P.; Yu, G.; Liu, Y. *J. Org. Chem.* **2008**, *73*, 594−602.
(33) Xia, R.; Lai, W.; Levermore, P. A.; Huang, W.; Bradley, D. D. C. *Adv. Funct. Mater.* **2009**, *19*, 2844−2850.
(34) Adams, M. J.; Highfield, J. G.; Kirkbright, G. F. *Anal. Chem.* **1977**, *49*, 1850−1852.
(35) de Mello, J. C.; Wittmann, H. F.; Friend, R. H. *Adv. Mater.* **1997**, *9*, 230−232.
(36) Shaklee, K. L.; Leheny, R. F. *Appl. Phys. Lett.* **1971**, *18*, 475−477.
(37) Kruzinauskiene, A.; Matoliukstyte, A.; Michaleviciute, A.; Grazulevicius, J. V.; Musnickas, J.; Gaidelis, V.; Jankauskas, V. *Synth. Met.* **2007**, *157*, 401−406.
(38) Lux, M.; Strohriegl, P.; Höcker, H. *Makromol. Chem.* **1987**, *188*, 811−820.
(39) Sonntag, M.; Kreger, K.; Hanft, D.; Strohriegl, P.; Setayesh, S.; de Leeuw, D. *Chem. Mater.* **2005**, *17*, 3031−3039.
(40) Dierschke, F.; Grimsdale, A. C.; Müllen, K. *Synthesis* **2003**, 2470−2472.
(41) Frisch, M. J.; Trucks, G. W.; Schlegel, H. B.; Scuseria, G. E.; Robb, M. A.; Cheeseman, J. R.; Montgomery, J. A., Jr.; Vreven, T.; Kudin, K. N.; Burant, J. C.; et al. *Gaussian 03, Revision D.01*; Gaussian, Inc.: Wallingford, CT, 2004; (for the complete reference, see the Supporting Information).
(42) Crawford, A. G.; Dwyer, A. D.; Liu, Z.; Steffen, A.; Beeby, A.; Pålsson, L.-O.; Tozer, D. J.; Marder, T. B. *J. Am. Chem. Soc.* **2011**, *133*, 13349−13362.
(43) Ramart-Lucas, M.; Matti, M. J.; Guilmart, T. *Bull. Soc. Chim. Fr.* **1948**, *15*, 1215−1225.
(44) Romero-Ale, E. E.; Olives, A. I.; Martín, M. A.; del Castillo, B.; López-Alvarado, P.; Menéndez, J. C. *Luminescence* **2005**, *20*, 162−169.
(45) Acar, N.; Kurzawa, J.; Fritz, N.; Stockmann, A.; Roman, C.; Schneider, S.; Clark, T. *J. Phys. Chem. A* **2003**, *107*, 9530−9541.
(46) Horrocks, D. L.; Brown, W. G. *Chem. Phys. Lett.* **1970**, *5*, 117−119.
(47) Birks, J. B. *Rep. Prog. Phys.* **1975**, *38*, 903−974.
(48) Winnik, F. M. *Chem. Rev.* **1993**, *93*, 587−614.
(49) Jones, G.; Vullev, V. I. *J. Phys. Chem. A* **2001**, *105*, 6402−6406.
(50) Saragi, T. P. I.; Spehr, T.; Siebert, A.; Fuhrmann-Lieker, T.; Salbeck, J. *Chem. Rev.* **2007**, *107*, 1011−1065.
(51) Zhao, Z.; Chen, S.; Lam, J. W. Y.; Lu, P.; Zhong, Y.; Wong, K. S.; Kwok, H. S.; Tang, B. Z. *Chem. Commun.* **2010**, *46*, 2221−2223.
(52) Bernhardt, S.; Kastler, M.; Enkelmann, V.; Baumgarten, M.; Müllen, K. *Chem.—Eur. J.* **2006**, *12*, 6117−6128.
(53) Tessler, N. *Adv. Mater.* **1999**, *11*, 363−370.
(54) Samuel, I. D. W.; Turnbull, G. A. *Chem. Rev.* **2007**, *107*, 1272−1295.
(55) Kazlauskas, K.; Tamulaitis, G.; Žukauskas, A.; Suski, T.; Perlin, P.; Leszczynski, M.; Prystawko, P.; Grzegory, I. *Phys. Rev. B* **2004**, *69*, 245316−245324.
(56) Miasojedovas, A.; Kazlauskas, K.; Armonaite, G.; Sivamurugan, V.; Valiyaveettil, S.; Grazulevicius, J. V.; Jursenas, S. *Dyes Pigm.* **2012**, *92*, 1285−1291.
(57) Tsutsumi, N.; Kawahira, T.; Sakai, W. *Appl. Phys. Lett.* **2003**, *83*, 2533−2535.
(58) Calzado, E. M.; Villalvilla, J. M.; Boj, P. G.; Quintana, J. A.; Gomez, R.; Segura, J. L.; Diaz-Garcia, M. A. *J. Phys. Chem. C* **2007**, *111*, 13595−13605.
(59) Calzado, E. M.; Boj, P. G.; Díaz-García, M. A. *Int. J. Mol. Sci.* **2010**, *11*, 2546−2565.